Robust Motion Planning of the Powered Descent of a Space Vehicle

Clara Leparoux, Bruno Hérissé, Frédéric Jean

Available online at www.sciencedirect.com

ScienceDirect

IFAC Papers Online CONFERENCE PAPER ARCHIVE

IFAC PapersOnLine 56-2 (2023) 2001–2006

Robust Motion Planning of the Powered Descent of a Space Vehicle

Clara Leparoux * **Bruno Hérissé** ** **Frédéric Jean** ***

* *DTIS, ONERA & UMA, ENSTA Paris (e-mail: clara.leparoux@ensta-paris.fr)*
** *DTIS, ONERA, Université Paris-Saclay, F-91123 Palaiseau, France (e-mail: bruno.herisse@onera.fr)*
*** *UMA, ENSTA Paris, Institut Polytechnique de Paris, 91120 Palaiseau, France (e-mail: frederic.jean@ensta-paris.fr)*

Abstract: The motion planning of powered descent problems has often been treated in the deterministic optimal control framework, which provides efficient theoretical and numerical tools. However, future applications require robustness, usually obtained by introducing stochastic components in the dynamics to model uncertainties. After stating the robust motion planning problem, this paper proposes a deterministic approximation which avoids the computational difficulties of stochastic optimal control. The approach consists of guiding the mean while reducing the covariance, the dynamics of these two quantities being approximated thanks to statistical linearization. In addition, since feedback control is necessary to control covariance, two techniques are provided to deal with actuator limits when the control is stochastic.

Keywords: Trajectory and Path Planning, Aerospace, Robust Control, Control of constrained systems.

1. INTRODUCTION

By the renewed interest these last years for Mars and Moon exploration, with new missions requiring high landing precision, and the growing use of reusable launchers, it has become necessary to devise efficient vertical landing strategies (Blackmore (2016)). A challenge in vertical landing is the final phase, the powered descent, which begins a few kilometers above the landing site with a limited amount of fuel remaining. Thus, feedback control is used to achieve the required landing accuracy using the available measurements. Its role is to track a reference trajectory computed by motion planning (Ganet-Schoeller and Brunel (2019)).

The motion planning has frequently been treated in an optimal control framework, seeking for the control succeeding to steer the vehicle to a target while minimizing a cost function. The existing litterature on powered descent problems (Meditch (1964), Lu (2018), Leparoux et al. (2022b)) found that optimal solutions have generally a Max-Min-Max form, which corresponds to a control of the engine throttle that switches twice between its maximum and minimum levels. This form of solution is well suited for rocket engines because it does not require thrust modulation. However, it is sensitive to perturbations and errors on the initial conditions, which may be significant when landing on planets other than Earth (Braun and Manning (2007)).

We account for these uncertainties with robust motion planning. In this paper, we focus on the modeling of perturbations and measurement errors. Therefore, we do not consider methods for robust motion planning that are suited for parameter uncertainties, such as robust set methods (Cheng et al. (2019)) or methods reducing the sensitivity of a performance criteria (Shen et al. (2010)). We prefer the stochastic approach, in which uncertainties are modeled by introducing a white noise into the dynamics and modeling the vehicle state as a random variable. Then, the robustness of the motion planning is ensured provided that dispersions around the mean trajectory are limited. This leads to a stochastic formulation of the motion planning problem, which is not desirable since few theoretical results exist and numerical methods in the stochastic optimal control framework are computationally heavy. In the literature, several references propose covariance control approaches through feedback control for linear dynamics. For instance, Chen et al. (2015) use a LQG regulator to steer the state of a linear system to a specified terminal Gaussian distribution. Moreover, Ridderhof and Tsiotras (2019) present an algorithm for powered descent that considers separately the mean steering which has the role to bring the vehicle to the target optimally, and the covariance steering to attain prescribed final dispersions. When considering non linear dynamics, Berret and Jean (2020) propose to approximate the motion planning solution by the one of an open-loop stochastic optimal control problem, by estimating the first two moments of the state thanks to statistical linearization.

Thus, it appears that leveraging feedback control to achieve robust motion planning through covariance control is promising. However, this requires to take into account actuator limits, usually modelled by control bounds. For the powered descent problem, several ideas have been proposed to handle them. For instance, in Shen et al. (2010),

10.1016/j.ifacol.2023.10.1095

the feedback gain is multiplied by a factor that vanishes when the nominal control is close to the control bounds. In Ridderhof and Tsiotras (2019), the control bounds are formulated as chance constraints and convexified. Moreover, Ridderhof and Tsiotras (2021) extend this approach by computing conservative margins that ensure control bounds are respected.

This paper proposes a robust motion planning approach for the powered descent problem, which considers a realistic space vehicle modeling with non linear dynamics, actuator limits and state constraints. It consists of approximating the solution by the one of a deterministic optimal control problem reducing the state covariance for robustness. Uncertainties are modeled following the stochastic approach. The dynamics of the mean and the covariance are approximated thanks to statistical linearization. In addition, we propose two different ways to manage actuator limits. Specifically, one of the proposed solutions consists of including a smooth approximation of the saturation function directly in the dynamics. Theoretical justifications of the approach are provided in a complementary work (Leparoux et al. (2023)).

This paper is organized as follows. First, we present the modeling of the landing problem considered. Then, we detail how we formulate a robust motion planning problem thanks to statistical linearization. In Section 4, we present how to incorporate actuator limits and state constraints, and finally Section 5 provides some numerical results.

2. FRAMEWORK

Let us study the motion planning of a space vehicle during the powered descent phase. It is treated here as an optimal control problem. Only the two dimensional case is considered. The aim is to compute a reference trajectory and a reference control that allow the space vehicle to reach a predefined target S_f while minimizing fuel consumption.

2.1 Deterministic landing problem

First, let us describe the unperturbed dynamics of the space vehicle, when assuming that all parameters are known and that the vehicle is only affected by its weight and by the engine thrust. The state is denoted $x = (r, v, m) \in \mathbb{R}^2 \times \mathbb{R}^2 \times \mathbb{R}$ where r is the position, v the velocity, m the mass of the vehicle. Its unperturbed dynamics are expressed by $\dot{x} = f(x, u)$ in an inertial frame (e_x, e_z), such that

$$\begin{cases} \dot{r} &= v, \\ \dot{v} &= \dfrac{T}{m}u - g_0, \\ \dot{m} &= -q\|u\|, \end{cases} \tag{1}$$

where $u \in \mathbb{R}^2$ is the control, q the maximal mass flow rate of the engine, $T > 0$ the maximal thrust and $g_0 = (0, g_a)$ with g_a the gravitational acceleration. The initial mass of the vehicle is denoted m_0 and its empty mass m_e. Technical limits and security requirements are modeled by state and control constraints, as explained in further details in Leparoux et al. (2022a). They should be satisfied for all $t \in [0, t_f)$ and are expressed by:

$$\begin{cases} m(t) > m_e \ , & (2) \\ 0 \leq u_{min} \leq \|u(t)\| \leq u_{max}, & (3) \\ \langle e_z, u(t)\rangle \geq \|u(t)\| \sin(\theta_{min}), \text{ with } \theta_{min} \in [0, \dfrac{\pi}{2}), & (4) \\ r_z(t) - \tan(\gamma)|r_x(t)| \geq 0, \text{ with } \gamma \in [0, \dfrac{\pi}{2}). & (5) \end{cases}$$

According to Leparoux et al. (2022a)[Theorem 1.1 and Proposition 4.3], for generic initial conditions, the optimal control u that steers (r, v) following (1) to zero under the constraints (2), (3), (4), (5) while maximizing the final mass has a Max-Min-Max form, i.e. there exist t_1 and t_2 with $0 \leq t_1 \leq t_2 \leq t_f$ such that

$$\|u(t)\| = \begin{cases} u_{max} \text{ if } t \in [0, t_1) \cup (t_2, t_f], \\ u_{min} \text{ if } t \in [t_1, t_2]. \end{cases} \tag{6}$$

2.2 Modeling of uncertainties

The above motion planning formulation expresses the problem of computing the cheapest way to attain a target. However, in the presence of perturbations and uncertainties, constraints might be violated, which could cause the failure of the mission. In order to take into account the uncertainties when computing the solution, we model them by introducing stochastic components in the problem. In the case of the powered descent problem, several uncertainties may act on the dynamics:

- uncertainties on the initial state, due to measurement errors and drifts on position and velocity estimates.
- perturbations of the dynamics, such as aerodynamic forces not modeled in (1). This is modeled by a white noise on the dynamics, such that
$$dx_t = f(x_t, u(t))dt + g(x_t)dW_t, \tag{7}$$
where x_t is a stochastic state variable, $g(x_t) = \frac{\sigma}{m_t}$ is a diffusion term and dW_t a monovariate Wiener process. However, we neglect the perturbations on the mass equation, by defining the standard deviation vector $\sigma \in \mathbb{R}^5$ with the last component equal to zero.

2.3 Robust motion planning

For now, we do not consider the state constraints (2) and (5). When considering a stochastic system, motion planning consists of imposing terminal constraints on the trajectory, typically imposing the mean to reach the target. Moreover, for the mean to be representative of the global behavior of the system, the dispersion of the sample trajectories must be small along the trajectories and at the final time. To this end, we add penalizations in the cost function on the integral of the covariance P_x along the trajectory and on the final covariance $P_x(t_f)$. Let us denote by $\mathcal{U} = \{u | u_{min} \leq \|u\| \leq u_{max} \text{ and } \langle e_z, u\rangle \geq \|u\| \sin(\theta_{min})\}$ the admissible control set. Then a first robust motion planning problem can be stated in a stochastic framework as follows

Problem 1. (Stochastic robust motion planning).

$$\min_{u, t_f} \quad \mathbb{E}[-m_{t_f}] + \mathrm{tr}(Q_f P_x(t_f)) + \int_0^{t_f} \mathrm{tr}(Q P_x(t))dt$$

under the constraints

$$\begin{cases} x_t \text{ follows (7)}, \\ u(t) \in \mathcal{U} \ \forall t \in [0, t_f), \\ \mathbb{E}[x_{t_f}] \in \mathcal{S}_f. \end{cases}$$

3. DETERMINISTIC PROBLEM APPROXIMATION

A stochastic optimal control problem such as Problem 1 is difficult to solve because few theoretical and numerical methods are available and they are computationally expensive. In this section, we propose a deterministic approximation of Problem 1.

3.1 Statistical linearization

As explained in Section 2.3, the quantities of major interest for motion planning are the first two moments of x_t. Thus we prefer working on an approximation of Problem 1 using as state variables the mean and the covariance, denoted respectively by m_x and P_x. We approximate m_x and P_x using a statistical linearization method, as solutions $(\hat{x}, P)$ of the following differential system

$$\begin{cases} \dot{\hat{x}} &= f(\hat{x}, u), \\ \dot{P} &= D_x f(\hat{x}, u)P + PD_x f(\hat{x}, u)^\top + g(\hat{x})g(\hat{x})^\top. \end{cases} \tag{8}$$

Statistical linearization methods have been used for a long time, especially in the fields of mechanics, and are well known. See for instance Berret and Jean (2020) for justifications of their use in motion planning. Thus, the control solution of Problem 1 is approximated by the control solution of the following problem

Problem 2. (Deterministic robust motion planning).

$$\min_{u, t_f} \quad -\hat{m}(t_f) + \mathrm{tr}(Q_f P(t_f)) + \int_0^{t_f} \mathrm{tr}(QP(t))dt \tag{9}$$

under the constraints

$$\begin{cases} (\hat{x}, P)(\cdot) \text{ follows (8)}, \\ u(t) \in \mathcal{U} \ \forall t \in [0, t_f), \\ \hat{x}(t_f) \in \mathcal{S}_f. \end{cases}$$

However, the viewpoint of Problems 1 and 2, and of any optimal control problem, is consistent only if there is accessibility. Indeed, if the covariance is not accessible, then there exists no solution substantially reducing it or even preventing it from increasing. Accessibility of statistically linearized systems has been studied in Bonalli et al. (2022), where a sufficient accessibility condition is clarified. We checked this condition for the launcher modeling described in this paper and it appears that it is not verified when considering (1) as dynamics. The calculation of the accessibility condition for the launcher example is too long to be presented in this paper. The details as well as theoretical justifications of the well-posedness of statistical linearization are provided in Leparoux et al. (2023).

Remark 3. Since the condition given in the reference is only sufficient, its calculation on the open-loop launcher dynamics does not prove that the linearized dynamics are not accessible. However, in light of numerical results such as simulations presented in the last section of this paper, it seems clear that it is difficult to keep the covariance small when considering controls only function of time.

3.2 Feedback for covariance control

Considering the open-loop dynamics (8) is not satisfying to solve Problems 1 and 2, as explained in Section 3.1. Since position and velocity measurements are available during the powered descent, we modify the launcher dynamics by the one obtained when considering u as a function of position and velocity. However, the mass is not considered in the feedback, because it is not observable in general and we assume that it is not measured. Let us note first that u represents the normalized thrust of an engine, whose force and direction are controlled by different actuators. Therefore, we adopt a notation of u, which separates its norm u_ρ and its direction u_θ, such that

$$u = u_\rho \begin{pmatrix} \cos(u_\theta) \\ \sin(u_\theta) \end{pmatrix} \tag{10}$$

where $u_\rho = \|u\|$ and $u_\theta \in [-\pi, \pi)$. Then, we assume that there are linear feedbacks on the norm and the direction, such that

$$u_{FB}(x, t) = (\rho(t) + K_n(t)\xi(t)) \begin{pmatrix} \cos(\theta(t) + K_d(t)\xi(t)) \\ \sin(\theta(t) + K_d(t)\xi(t)) \end{pmatrix} \tag{11}$$

where ρ and θ are deterministic references, K_n and $K_d \in \mathbb{R}^4$ feedback gains, and $\xi = (r, v)$ is a reduced state vector. Finally, we will seek to solve Problem 2 where the dynamics (7) that we approximate by statistical linearization (8) have the following unperturbed dynamics

$$f_{FB}(x, u(t)) = f(x, u_{FB}(x, t)). \tag{12}$$

Remark 4. There are other advantages in considering feedback controls in motion planning, particularly when seeking robustness. Indeed, motion planning is used for providing a reference to a tracking controller, generally achieved using feedback control. By incorporating the feedback into motion planning, we obtain reference feedback gains which can be used to initialize the computations of real feedback gains. Moreover, actuator limits can be planned or avoided, as detailed further in the next section. The main drawback of considering feedback controls is their cost, since they require sensors or observers to acquire measurements, and processing to be operable.

However, a difficulty arises when assuming a control as (11) in Problem 2, because we cannot consider a stochastic control constraint such as $u_{BF}(x) \in \mathcal{U}$. The next Section will present how to deal with control constraints.

4. CONSIDERATION OF ACTUATOR LIMITS AND STATE CONSTRAINTS

In this section, we detail how to include in Problem 2 the control and state constraints presented in Section 2.1 when assuming (12) as unperturbed dynamics. First, we present saturations as the actual modeling of actuator limits. Then we detail two approaches to handle these saturations in the motion planning problem and finally we deal with state constraints.

4.1 Saturated dynamics modeling

The launcher modeling, which is described in Section 2.1, is well-suited for the purpose of motion planning. In fact, the control constraints presented in equations (3) and (4) are a representation of actuator limits, which are an integral part of the system dynamics. Define the following saturation function

$$\text{sat}_a^b(x) = \begin{cases} a \text{ if } x < a, \\ b \text{ if } x > b, \\ x \text{ otherwise.} \end{cases} \tag{13}$$

Then, using the notation of the control introduced by (10), a more accurate description of the vehicle unperturbed dynamics can be expressed as

$$f_{sat}(x,u) = f\left(x, \text{sat}_{u_{min}}^{u_{max}}(u_\rho)\begin{pmatrix}\cos(\text{sat}_{\theta_{min}}^{\pi-\theta_{min}}(u_\theta)) \\ \sin(\text{sat}_{\theta_{min}}^{\pi-\theta_{min}}(u_\theta))\end{pmatrix}\right). \tag{14}$$

However, this description leads to non-smooth dynamics, which makes it unsuitable for statistical analysis. In the subsequent two subsections, we propose alternative approaches to incorporate actuator limits which are well-suited for statistical linearization.

4.2 Actuator limits as chance constraints

A common way to deal with actuator limits in the presence of a feedback is to formulate them as chance constraints. Thus, the control solution should stay away from the bounds with a margin depending on the estimation of the level of uncertainties and a chosen success probability threshold. Let us formulate the norm and direction constraints. First, consider the norm constraint (3) such that for all $t \in [0, t_f)$

$$\Pr(u_{min} \leq u_\rho \text{ and } u_\rho \leq u_{max}) > p_n \ . \tag{15}$$

Then, considering the direction constraint (4), we impose with a threshold p_d that for all $t \in [0, t_f)$

$$\Pr\left(\sin(u_\theta) \geq \sin(\theta_{min})\right) > p_d \ . \tag{16}$$

Chance constraints are well suited for statistically linearized system, since, under a Gaussian distribution hypothesis, they can be reformulated into deterministic constraints on the mean and the covariance, thanks to the following common result that we recall.

Let us consider a chance constraint such as

$$\Pr[a^\top x \leq c] \geq p, \tag{17}$$

where $x \in \mathbb{R}^n$ is a stochastic variable Gaussian distributed of mean m_x and covariance P_x, $a \in \mathbb{R}^n$, c a constant and p a probability threshold. Then, (17) is equivalent to

$$a^\top m_x + \Psi^{-1}(p)\sqrt{a^\top P_x a} \leq c, \tag{18}$$

where Ψ^{-1} is the inverse cumulative distribution function of the normal distribution. Therefore, (15) is equivalent to

$$\begin{aligned} u_{max} - (\rho(t) + K_n(t)\hat{\xi}(t)) \geq \\ \Psi^{-1}(p_n)\sqrt{K_n(t)\overline{P}(t)K_n(t)^\top} \ , \\ \text{and} \\ (\rho(t) + K_n(t)\hat{\xi}(t)) - u_{min} \geq \\ \Psi^{-1}(p_n)\sqrt{K_n(t)\overline{P}(t)K_n(t)^\top} \ ; \end{aligned} \tag{19}$$

and (16) is equivalent to

$$\begin{aligned} (\pi - \theta_{min}) - (\theta(t) + K_d(t)\hat{\xi}(t)) \geq \\ \Psi^{-1}(p_d)\sqrt{K_d(t)\overline{P}(t)K_d(t)^\top} \ , \\ \text{and} \\ (\theta(t) + K_d(t)\hat{\xi}(t)) - \theta_{min} \geq \\ \Psi^{-1}(p_d)\sqrt{K_d(t)\overline{P}(t)K_d(t)^\top} \ ; \end{aligned} \tag{20}$$

where $\overline{P} \in \mathcal{M}_4(\mathbb{R})$ is a matrix composed of the first four lines and columns of P. The disadvantage of this modeling is that the constraints can be numerically hard to handle, since (19) and (20) constrain both the mean and the covariance.

4.3 Smooth approximation of the saturation function

We propose an other approach that amounts to consider (14) as dynamics with (11) as control. This requires to approximate the saturated dynamics by smooth functions in order to make them tractable. Let us recall first that (13) can be explicited as

$$\text{sat}_a^b(x) = \frac{b+a}{2} + \frac{|x-a| - |x-b|}{2}. \tag{21}$$

Therefore (13) can be approximated smoothly by replacing absolute values in (21) following

$$|x| \sim \sqrt{x^2 + \epsilon^2}, \tag{22}$$

the approximation being all the more accurate as the parameter $\epsilon > 0$ is close to zero.

4.4 State constraints

The state constraints given by (2) and (5) indicate that any violation of these constraints would result in a failure of the motion planning problem due to a significant change in the system dynamics. Indeed, the violation of (2) would force the control to zero, and assuming that the violation of (5) would cause a crash, then in that situation the entire dynamics of the vehicle would be zero. Therefore, we formulate the motion planning problem to ensure that these constraints are satisfied with a chosen level of confidence. To do this, when considering hazards, we impose constraints on the mean with conservative deterministic margins. Considering the mass constraint (2), this leads to

$$\hat{m}(t) > (1+\eta)m_e \ \forall t \in [0, t_f), \tag{23}$$

where η is a margin greater than the order of magnitude of the uncertainties on mass measurements. Considering the glide-slope constraint (5), this leads to

$$\hat{r}_z - \tan(\gamma)|\hat{r}_x| \geq 0. \tag{24}$$

The robustness of the satisfaction of the glide-slope-constraint is ensured by taking γ sufficiently high.

Remark 5. Chance constraint formulations could be used to include state constraints too. However, it would require to change the definition of the glide-slope constraint, by taking a constraint cone of vertex at lower altitude than the target, so that it does not conflict with the terminal constraint. A probability formulation for the mass constraint is also possible, but we prefer not to add a constraint on the mass variance since there is no feedback on the mass.

5. NUMERICAL RESULTS

Now, let us present some examples of motion planning for the powered descent problem, illustrating the different formulations presented in this paper. Computations, based on a direct method, are performed using CasADi (Andersson et al. (2019)) with Python language and the IPOPT solver. For time discretization of the considered

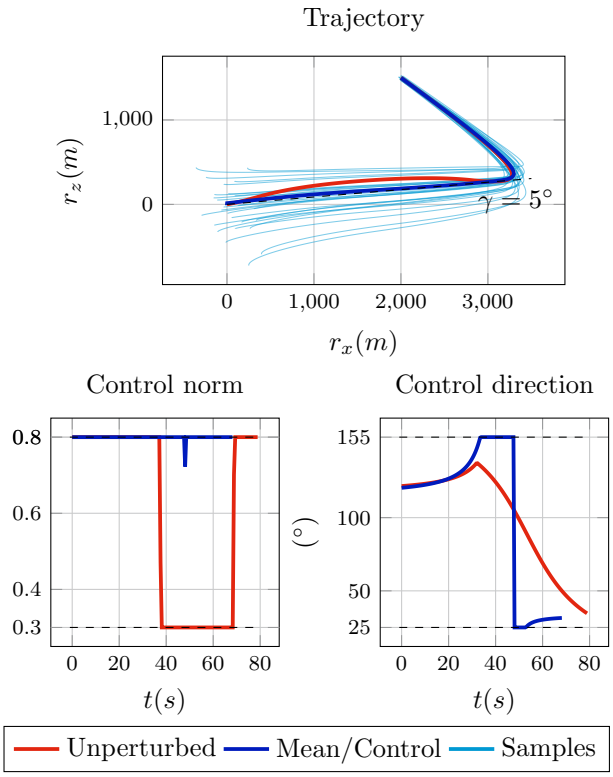

Fig. 1. Simulations of random trajectories with an open loop control

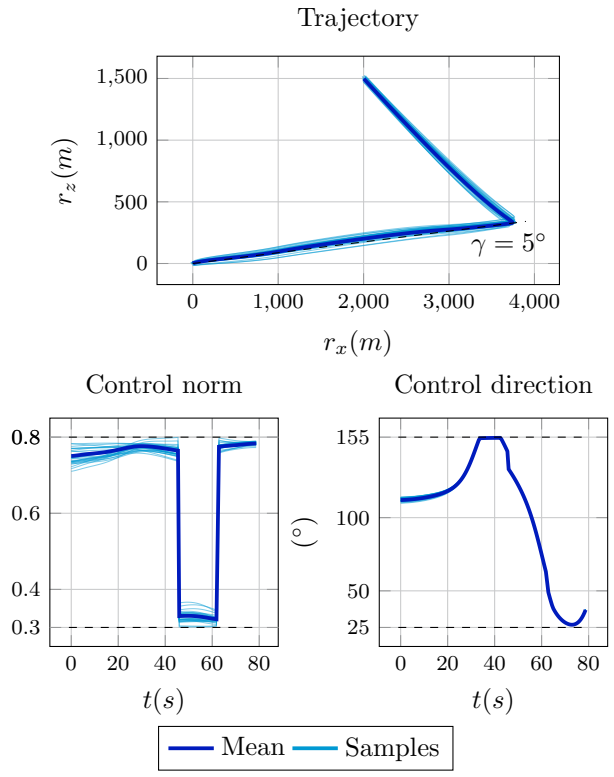

Fig. 2. Simulations of random trajectories minimizing the covariance, with actuator limits as chance constraints

optimal control problems, a grid of 150 nodes is used. The vehicle parameters are $T = 16573N$, $u_{min} = 0.3$, $u_{max} = 0.8$, $q = 8.4294kg/s$ and $m_e = 1350kg$. The parameter $g_a = 3.71m/s^2$ corresponds to the Earth gravitational constant. The goal is to steer the vehicle to zero final position and velocity, and the final time t_f is free. The initial mean state is given by $x_0 = (2000m, 1500m, 100m/s, -75m/s, 1905kg)$. The initial covariance matrix is set in order to model measurement uncertainties of the initial state, assumed to be Gaussian, such that $P^0 = \text{diag}(200m^2, 200m^2, 10(m/s)^2, 10(m/s)^2, 361kg^2)$. Along the trajectory, the dynamics are subject to perturbations of dispersion $\sigma = (0, 0, 100N, 10N, 0)$. The pointing constraint angle is $\theta_{min} = 25°$ and the glide slope angle $\gamma = 5°$. The dynamics of the launcher are such that the mass covariance changes little along the trajectory. Therefore, we fix the mass margin to a conservative value $\eta = 3.7\%$ such that ηm_e is superior to two times the initial mass dispersion. To generate the results, the following approach was applied: first the solution of Problem 2 was calculated with $Q = \text{diag}(200, 200, 100, 100)$ and $Q_f = \text{diag}(1000, 2000, 100, 100)$. We do not penalize the mass variance since there is no feedback on the mass. Then the dynamics (8) were simulated using the computed reference controls and feedback gains, and the resulted trajectories and controls are plotted. The deterministic fuel saving optimal solution for $Q = Q_f = 0$ is shown in red on the first set of plots for comparison.

Fig. 1 shows in blue trajectories generated by the solution of Problem 2, which is depicted below, when considering an open-loop control. The norm of the control solution is almost always saturated, and the final time $t_f = 68.2s$ is smaller than in the deterministic case ($t_f = 78.9s$). This seems to be a consequence of the lack of accessibility of the covariance, which forces the solution to choose another way to limit its growth by reducing the duration of the trajectory. Therefore, it is not surprising that covariance stays high, with a final position and velocity standard deviation of $(233.9m, 259.5m, 3.2m/s, 5.0m/s)$. Fig. 2 shows trajectories generated by the control solution when considering feedback dynamics and using chance constraints ($p_n = p_d = 0.99$) to handle actuator limits. Then, the cost function is now the sum of (9) and a penalization of the feedback gains and their derivatives:

$$\min_{\rho,\theta,K_n,K_d,t_f} \quad -\hat{m}(t_f) + \text{tr}(Q_f\overline{P}(t_f)) + \int_0^{t_f} \text{tr}(Q\overline{P}) \\ +0.5(\|K_n\|^2 + \|K_d\|^2 + \|\dot{K}_n\|^2 + \|\dot{K}_d\|^2)dt. \tag{25}$$

The dispersion is controlled all along the trajectory, and the final state standard deviation is $(12.2m, 9.7m, 1.4m/s, 1.0m/s)$, and $t_f = 78.7s$. Finally, Fig. 3 shows trajectoires generated by the solution when considering feedback controls and a smooth modeling of actuator limits, with $\epsilon = 0.02$ for the norm saturation and $\epsilon = 0.0002$ for the direction. The cost is still expressed by (25). The final state standard deviation is $(12.8m, 9.9m, 1.2m/s, 0.9m/s)$ and the final time $t_f = 80.4s$.

Remark that the two stochastic controls are alike the deterministic solution, regarding the shape and the duration, except that there are margins between the extreme values of the control and the real values of actuator bounds u_{min} and u_{max}. By setting the probability parameters p_n and p_d to larger values in the second approach and the ϵ parameters in the third approach, we would obtain solutions with larger margins, which would ensure better

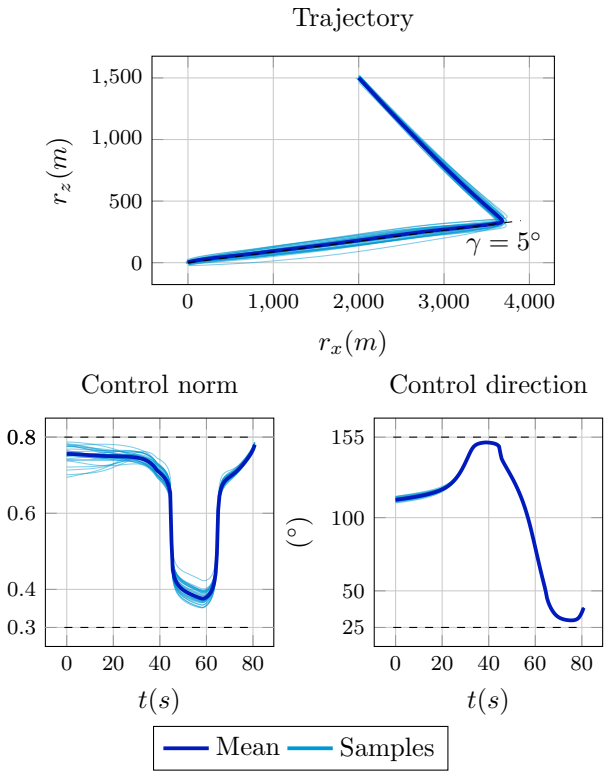

Fig. 3. Simulations of random trajectories minimizing the covariance, with a smooth modeling of actuator limits

robustness with respect to the control bounds. However, this may cause convergence issues, especially for the chance constraints approach. Here, the third solution takes larger margins from the bounds, while attaining similar final dispersions. Moreover, since the ϵ parameter in the third approach influences the smoothness of the solution, it can be adjusted so that the reference control fits realistic engine dynamics. Finally, the smoothly saturated dynamics approach is adaptable outside the context of statistical linearization since it only requires estimations of the mean to compute the control margins, while in the chance constraints approach the margins depend on both mean and covariance estimations.

6. CONCLUSION

In this paper, we have presented a robust motion planning method using statistical linearization and applied it to a powered descent problem. The vehicle dynamics representation considers a feedback form of control, based on two crucial observations: first, limiting the covariance is essential to ensure the robustness of the solution, and second, it requires the control to depend on the state. Moreover, we propose several ways to take into account actuator limits and state constraints, and justify our approach by numerical results. A comparative analysis of our method and established techniques could be conducted in future research, as well as a study for non Gaussian noise.

REFERENCES

Andersson, J.A.E., Gillis, J., Horn, G., Rawlings, J.B., and Diehl, M. (2019). CasADi – A software framework for nonlinear optimization and optimal control. *Mathematical Programming Computation*, 11(1), 1–36.

Berret, B. and Jean, F. (2020). Efficient computation of optimal open-loop controls for stochastic systems. *Automatica*, 115, 108874.

Blackmore, L. (2016). Autonomous precision landing of space rockets. *The Bridge*, 46(4), 15–20.

Bonalli, R., Leparoux, C., Hérissé, B., and Jean, F. (2022). On the accessibility and controllability of statistical linearization for stochastic control: Algebraic rank conditions and their genericity. ArXiv preprint arXiv:2207.10944.

Braun, R.D. and Manning, R.M. (2007). Mars exploration entry, descent, and landing challenges. *Journal of Spacecraft and Rockets*, 44(2), 310–323.

Chen, Y., Georgiou, T., and Pavon, M. (2015). Optimal control of the state statistics for a linear stochastic system. 54th IEEE Conference on Decision and Control.

Cheng, L., Wen, H., and Jin, D. (2019). Uncertain parameters analysis of powered-descent guidance based on chebyshev interval method. *Acta Astronautica*, 162, 581–588.

Ganet-Schoeller, M. and Brunel, A. (2019). Optimal guidance for 1st stage launcher recovery. *IFAC-PapersOnLine*, 52(12), 532–537.

Leparoux, C., Bonalli, R., Hérissé, B., and Jean, F. (2023). Statistical Linearization for Robust Motion Planning. ArXiv preprint arXiv:2303.01288.

Leparoux, C., Hérissé, B., and Jean, F. (2022a). Optimal planetary landing with pointing and glide-slope constraints. 61th IEEE Conference on Decision and Control.

Leparoux, C., Hérissé, B., and Jean, F. (2022b). Structure of optimal control for planetary landing with control and state constraints. *ESAIM: COCV*, 28, 67.

Lu, P. (2018). Propellant-optimal powered descent guidance. *Journal of Guidance, Control, and Dynamics*, 41(4), 813–826.

Meditch, J. (1964). On the problem of optimal thrust programming for a lunar soft landing. *IEEE Transactions on Automatic Control*, 9(4), 477–484.

Ridderhof, J. and Tsiotras, P. (2019). Minimum-fuel powered descent in the presence of random disturbances. AIAA Scitech 2019 Forum.

Ridderhof, J. and Tsiotras, P. (2021). Minimum-fuel closed-loop powered descent guidance with stochastically derived throttle margins. *Journal of Guidance, Control, and Dynamics*, 44(3), 537–547.

Shen, H., Seywald, H., and Powell, R.W. (2010). Desensitizing the minimum-fuel powered descent for mars pinpoint landing. *Journal of Guidance, Control, and Dynamics*, 33(1), 108–115.